

# Multi-scale measurement of acoustic particle velocity and flow velocity for liner investigations

D. Haufe · A. Fischer · J. Czarske ·  
A. Schulz · F. Bake · L. Enghardt

Received: 7 January 2013 / Revised: 13 June 2013 / Accepted: 18 June 2013 / Published online: 27 June 2013  
© Springer-Verlag Berlin Heidelberg 2013

**Abstract** The optimization of liners for noise reduction lacks a thorough comprehension of the inherent aeroacoustic damping phenomena. Therefore, the interaction of the acoustic particle velocity (APV) and the flow velocity field at liners has to be investigated. Hence, the simultaneous measurement of both quantities, differing by several orders of magnitude, is aspired. However, the required high dynamic range is challenging. In order to analyse the energy transfer from the acoustic wave to the flow turbulence, turbulence spectra must be resolved which necessitates a high measurement rate as well. Doppler global velocimetry with sinusoidal laser frequency modulation (FM-DGV) fulfils these demanding requirements. First, the capability of FM-DGV for APV measurements was successfully validated with microphone measurements. Finally, a multi-point measurement at a bias flow liner was performed with a high dynamic range of 7,000 and a high measurement rate of 50 kHz. Hence, a deeper understanding of the aeroacoustics at liners can be gained in future investigations.

## 1 Introduction

The European Commission (2001) has aimed for reducing the noise emitted by aircraft by 10 dB until 2020 which corresponds to a reduction by about 50 % of the perceived noise level. To achieve this ambitious aim, silencing of the aircraft engines is indispensable. For that reason, liners, i.e., perforated walls with cavities behind representing Helmholtz resonators are applied in the engine. To increase their efficiency, an additional air stream can be directed through the perforations, the so-called bias flow, that interacts with the acoustic wave resulting in a decreased noise emission, see Eldredge and Dowling (2003). Bias flow liners are also employed in order to damp thermoacoustic instabilities affecting the functionality of gas turbine combustion systems, e.g., in Rupp et al. (2010), Jayatunga et al. (2012).

However, optimizing these bias flow liners is challenging due to the insufficient comprehension of the interaction between the flow and the sound. To obtain a deeper understanding of this interaction, the flow velocity and the acoustic particle velocity (APV) field at a bias flow liner have to be investigated. Since the effort of a simulation of such aeroacoustic scenario is tremendous due to the disparity of the scales, see Wang et al. (2006) and De Roeck et al. (2007), simultaneous measurements of both the flow velocity and the APV are pursued, for example, by Heuwinkel et al. (2010). However, a multi-scale measurement is essential, since the measurands have very different scales: consider, for example, an APV amplitude of about 7 mm/s corresponding to a sound pressure level (SPL) of 100 dB in a flow with a velocity of 30 m/s corresponding to a Mach number of about 0.1. The resulting needed dynamic range of about 4,000 is challenging. In addition, a high measurement rate is

---

D. Haufe (✉) · A. Fischer · J. Czarske  
Laboratory for Measurement and Testing Techniques,  
TU Dresden, Helmholtzstr. 18, 01069 Dresden, Germany  
e-mail: daniel.haufe@tu-dresden.de

A. Schulz  
Institute of Fluid Dynamics and Technical Acoustics,  
TU Berlin, Müller-Breslau-Str. 8, 10623 Berlin, Germany

F. Bake · L. Enghardt  
Institute of Propulsion Technology, DLR Berlin,  
Müller-Breslau-Str. 8, 10623 Berlin, Germany

required to resolve turbulence spectra allowing the analysis of the energy transfer from the acoustic wave to the flow turbulence. Moreover, the desired measurement technique is contactless which especially enables measurements also in a hot gas environment in order to study damping effects under conditions like in combustion chambers. Due to these demanding requirements for the measurement technique, only few optical measurements have been performed at liners until today.

Particle image velocimetry, e.g., has been used in Marx et al. (2010), Heuwinkel et al. (2010), Fischer et al. (2008), but suffers from an insufficient dynamic range which is typically about 200 (Raffel et al. 1998, p. 207). Laser Doppler anemometry was also applied by Minotti et al. (2008), Heuwinkel et al. (2010), but allows point-wise measurements only; thus, time-consuming traversing is necessary to obtain a velocity field. In contrast, Doppler global velocimetry with sinusoidal frequency modulation (FM-DGV) offers both the high dynamic range and the high measurement rates as well as a multi-point measurement as shown in Haufe et al. (2012). However, a validation of the APV measurement in a flow by means of FM-DGV is still missing. Furthermore, FM-DGV was not applied for liner investigations so far.

For that reason, measurements of the APV at a bias flow liner by means of FM-DGV are presented in this paper. Firstly, the measurement method FM-DGV is discussed briefly in Sect. 2. Secondly, the acoustic test rig especially designed for the measurements is described in Sect. 3. A validation of the APV measurement is accomplished by microphone measurements, see Sect. 4. Finally, two-dimensional vector measurements of the APV and the flow velocity at a bias flow liner are presented in Sect. 5. The paper closes with a conclusion in Sect. 6 where an outlook on further investigations is also given.

## 2 Measurement method

The measurement principle of FM-DGV is already explained thoroughly by Müller et al. (2007), Fischer et al. (2007). Thus, it is described only briefly here: the measurement of the velocity is based on evaluating the Doppler frequency shift of light scattered by small particles being added to the flow. The particles are assumed to have the same velocity as the flow. The particles are illuminated by laser light from the direction  $\mathbf{i}$ , as depicted in Fig. 1. The scattered light is observed in the direction  $\mathbf{o}$ , its Doppler frequency is obtained by means of spectroscopy using a molecular absorption cell and a photo detector. Evaluation of the detector signal gives an estimation for the Doppler frequency which corresponds to the velocity component  $v_{\text{meas}}$  in the direction  $\mathbf{o} - \mathbf{i}$ . Due to the sinusoidal

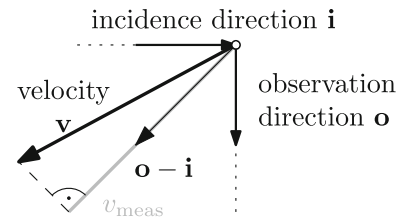


**Fig. 1** Velocity component  $v_{\text{meas}}$  measured by FM-DGV

modulation of the laser frequency with a modulation frequency up to 100 kHz, a maximum velocity measurement rate of 100 kHz can be achieved, see Fischer et al. (2009). The measurement range is maximum  $\pm 260$  m/s. By using a detector array, simultaneous measurements at multiple locations can be achieved. In order to obtain all three components of the velocity vector, three different observation directions  $\mathbf{o}$  or three illumination directions  $\mathbf{i}$  have to be used.

Finally, the amplitude  $v_{\text{ac}}$  and phase  $\varphi_{\text{ac}}$  of the APV as well as the mean flow velocity  $v_0$  are obtained using the Fourier transform of the measured velocity time series. The standard measurement uncertainty of the APV amplitude is discussed in Haufe et al. (2012) and amounts to typically about 4.5 mm/s for a measurement duration of 1 s with the present FM-DGV system, considering random deviations only. The standard uncertainty

$$\sigma_{\hat{v}_{\text{ac}}} \propto \frac{1}{\sqrt{T}} \quad (1)$$

can be reduced by increasing the measurement duration  $T$  due to averaging.

## 3 Measurement object

The measurement object is a flow duct called DUCT-R (Duct acoustic test rig with rectangular cross section) and was especially designed and built for the qualification of liner measurement techniques at the German Aerospace Center (DLR), Berlin in 2012. A drawing of the duct is depicted in Fig. 2, the duct has a length of 3.34 m and its cross section is 60 mm  $\times$  80 mm. While the walls are predominantly made of aluminium, the measurement section provides optical access through three glass windows (one at each side and one at the top). A radial compressor is used to generate the air flow from the left side of the picture with a maximum Mach number of 0.3. The sound was generated by a MONACOR speaker KU-516 located at the upstream section. The resulting SPL is maximum 134 dB. The end of the upstream section (left in Fig. 2) is connected to an anechoic termination to suppress undesired sound reflections.

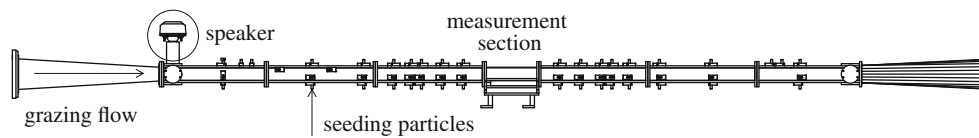


**Fig. 2** Drawing of the measurement object DUCT-R (*side view*)

#### 4 Measurement validation

For validation of the APV measurement in a flow by means of FM-DGV, acoustic plane waves are used and reference measurements with the established microphone technique were accomplished. In order to obtain plane waves only, a hard-walled measurement object and a sound frequency below the lowest cut-off frequency (Crocker 1998, p. 87) of higher-order modes, which is about 2.2 kHz here, were used. As a reference, flush-mounted condenser microphones have been used for simultaneously measuring the sound pressure at 14 positions along the axis of the duct. This allows the calculation of the sound pressure field by means of a decomposition of the sound field into forward and backward travelling waves, as described in Lahiri et al. (2011). Finally, the resulting APV amplitude profile in the duct was calculated using the linearized Euler equation (Rossing 2007, p. 216). To demonstrate the capabilities of FM-DGV, variable flow velocities with a Mach number from  $M_g = 0.02, \dots, 0.27$ , with a variable SPL at an arbitrarily chosen sound frequency  $f_{ac}$  of 683 Hz have been generated.

##### 4.1 Setup

The FM-DGV system used here is already described in detail in Fischer et al. (2009). Notwithstanding this description, the laser has been replaced by a new continuous-wave laser from TOPTICA Photonics with an optical amplifier providing an increased output power of 600 mW (previous model: 126 mW) in order to increase the scattering light power leading to a reduced measurement uncertainty, as proposed in Fischer et al. (2009). Scattering particles of diethylhexyl sebacate (DEHS) were generated by a PivPart40 aerosol generator from PIVTEC and inserted into the duct through holes at the side walls within the upstream section of the duct. The DEHS particles have a diameter of about 1  $\mu\text{m}$  and take the fluid velocity with a negligible slip which is lower than 1 % below 6.7 kHz (Albrecht et al. 2003, p. 608). The detection of the scattered light was achieved by a linear array of 25 fibre-coupled avalanche photo detectors allowing a simultaneous measurement at 25 locations at the duct (see Fig. 3) with a measurement rate of 50 kHz. Because of the limited number of digitizing channels of the data acquisition cards, only the signals of the 23 central detectors were acquired,

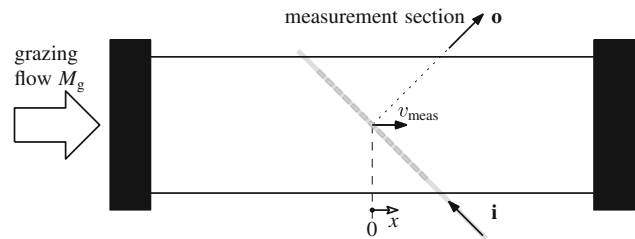


**Fig. 3** Measurement of the velocity  $v_{\text{meas}}$  at multiple locations at the hard-walled measurement object (*top view*)

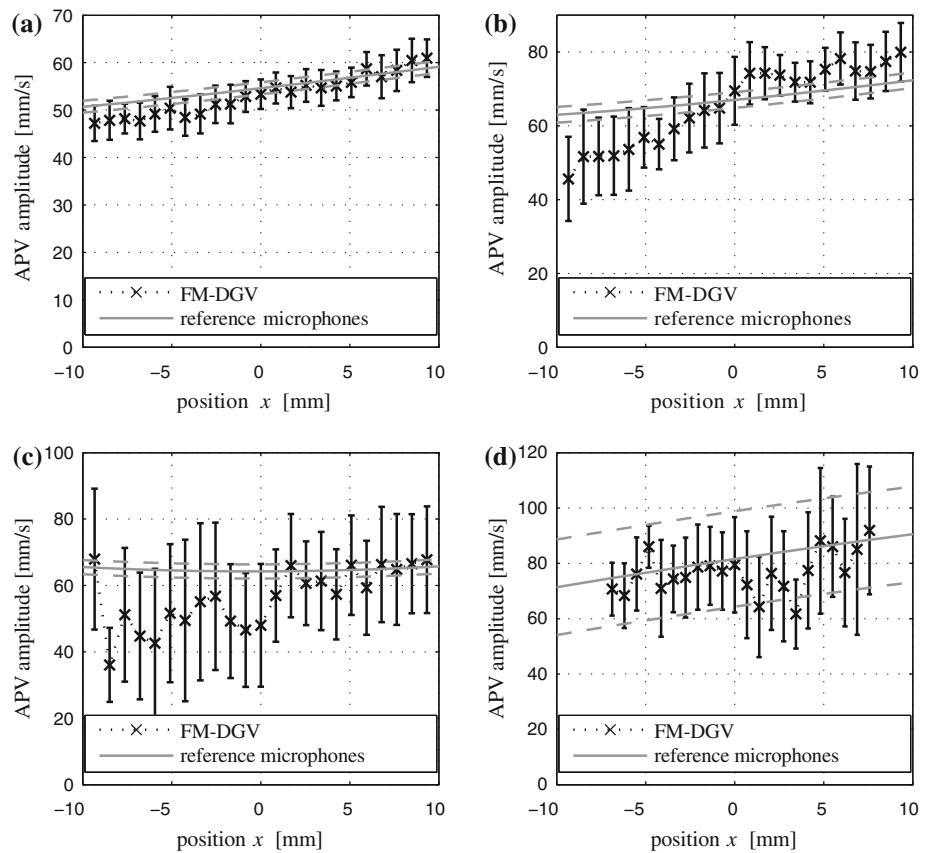
which is, however, satisfactory for the validation. To reduce the standard uncertainty, according to Eq. (1), ten repeated measurements were accomplished, each having a duration of 8 s. These 8 s are the maximum continuous measurement duration, which is limited by the memory of the data acquisition cards. According to Sect. 2, the measured component  $v_{\text{meas}}$  is orientated along the bisecting line of  $-\mathbf{i}$  and  $\mathbf{o}$  which is parallel to the axis of the duct here. Since plane waves propagating along the axis of the duct are assumed,  $v_{\text{meas}}$  comprises the whole magnitude of the expected APV vector. The spatial resolution is given by the shape of the measurement volume at each of the measurement locations, which can approximately be considered as a cylinder with a diameter of about 0.5 mm (given by the diameter of the laser beam) and a height of about 1 mm (given by the diameter of the imaging optics) orientated in the direction of  $\mathbf{i}$ . The spatial resolution is much smaller than the acoustic wavelength; thus, the acoustic wave can be resolved.

##### 4.2 Results

Examples for the results of the measured APV amplitude profile in the duct along the direction  $x$  are depicted in Fig. 4, including the 95 % confidence intervals (CIs), using Student's  $t$ -distribution assuming an approximately normal distribution. Each measured APV amplitude was obtained according to Sect. 2. The SPL is noted as the maximum SPL in the duct. For comparison, the APV amplitude profile resulting from the reference microphone measurement is also depicted in order to validate the measurements. A good agreement was achieved.

The standard uncertainty for a measurement duration of  $T = 80$  s and  $f_{ac} = 683$  Hz increases for higher flow velocities, from 1.4 mm/s in the case of  $M_g = 0.02$  to

**Fig. 4** APV amplitudes, measured with FM-DGV and validation with reference microphones. **a**  $f_{ac} = 683$  Hz, SPL: 122 dB,  $M_g = 0.02$ . **b**  $f_{ac} = 683$  Hz, SPL: 125 dB,  $M_g = 0.10$ . **c**  $f_{ac} = 683$  Hz, SPL: 125 dB,  $M_g = 0.19$ . **d**  $f_{ac} = 683$  Hz, SPL: 127 dB,  $M_g = 0.27$



about 11.4 mm/s for  $M_g = 0.25$ . The reason for this is the differing power spectral density (PSD) of the velocity, which is explained in the following: the PSD was additionally obtained by means of a Fourier transform of the velocity data from the FM-DGV measurement. Due to the high measurement rate of 50 kHz, the spectral range up to 25 kHz (Nyquist frequency) is resolved. The one-sided power spectral density  $2S_v(f)$  of the velocity is shown in Fig. 5a for  $M_g = 0.02$ – $0.25$ . The PSD was obtained by using the measured velocity data of ten repeated measurements with a continuous duration of 8 s each, which yields a frequency resolution of 1/8 Hz. To reduce random fluctuations of the estimated PSD, finally, an averaging of 16 frequency points has been applied, resulting in a final frequency resolution of 2 Hz, which is considered to be sufficiently fine.

Obviously,  $S_v(f)$  increases for faster flows, i.e., for higher Mach number  $M_g$  because of higher turbulent oscillations. These oscillations also cause a higher  $S_v(f_{ac})$  at the sound frequency  $f_{ac} = 683$  Hz superposing the APV amplitude. Hence, the stochastic oscillation affects the measured APV amplitude at  $f_{ac}$  more intensively for higher Mach numbers. This yields both an estimation bias of the APV amplitude, which is discussed in Haufe et al. (2012), and a higher standard uncertainty  $\sigma_{\hat{v}_{ac}}$  of the measured APV

amplitude  $\hat{v}_{ac}$ . Applying Parseval’s theorem for the stochastic portion of the signal, the standard uncertainty reads

$$\sigma_{\hat{v}_{ac}} = \lim_{\epsilon \rightarrow \pm 0} \sqrt{\frac{2S_v(f_{ac} + \epsilon)}{T}}, \tag{2}$$

whereby it is mandatory that  $\epsilon \neq 0$  holds in order to exclude the deterministic APV signal. If  $S_v(f_{ac})$  contained no deterministic signals, i.e., stochastic portions only, Eq. (2) would also be valid for  $\epsilon = 0$  which equals Zhou and Giannakis (1995). To prove Eq. (2), the standard uncertainty  $\sigma_{\hat{v}_{ac}}$  was compared to the sample standard deviation, calculated directly from the APV amplitude samples. The comparison of both results is depicted in Fig. 5b for  $x = 0$  and shows a good agreement. It should be mentioned that  $S_v(f)$  in Fig. 5a converges for high  $f$  to the noise PSD resulting from the measurement uncertainty, assuming ideal band-limited white noise, see Fischer et al. (2009). This is especially visible for  $M_g \leq 0.1$ , where less turbulent oscillations occur. The different noise PSDs (dashed lines in Fig. 5a) for  $M_g = 0.02$  and  $M_g = 0.1$  correspond to a different measurement uncertainty that depends on the scattering light power which deviated between the experiments. There are also spikes in the frequency range of 1 kHz to 2 kHz which are believed to result from the electronics used for the laser stabilization.

**Fig. 5** Results for variable number  $M_g$  of the flow and sound excitation at a frequency of  $f_{ac} = 683$  Hz for  $x = 0$  and  $T = 80$  s. **a** One-sided power spectral density. **b** Comparison of standard uncertainty

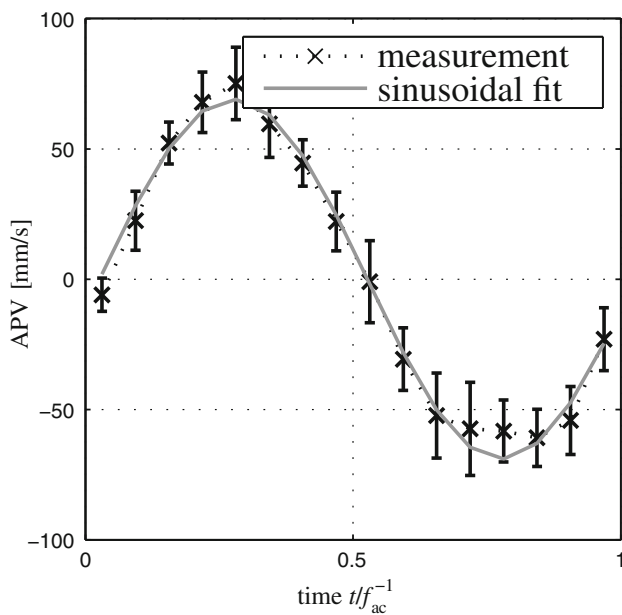
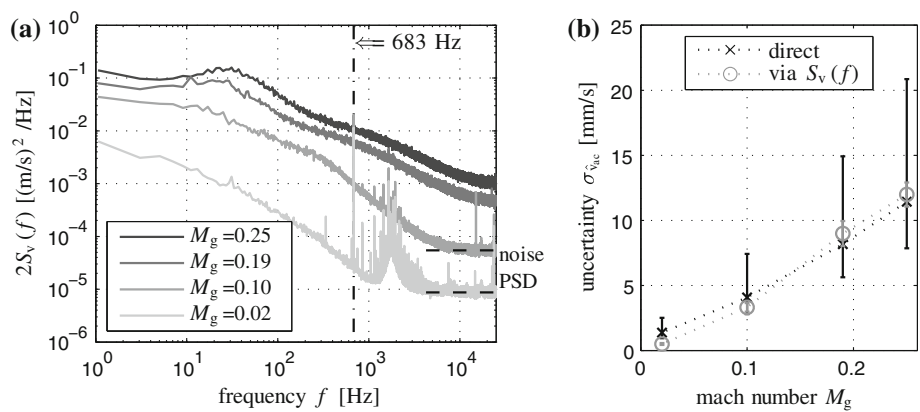


**Fig. 6** Time-resolved APV for  $f_{ac} = 683$  Hz, SPL: 125 dB,  $M_g = 0.10$  at  $x = 0$

In addition, the high measurement rate of 50 kHz enables the time-resolved measurement of the APV. Therefore, the zero-mean velocity time signal was split into 16 groups of almost equal acoustic phase with a phase resolution of  $\pi/8$  rad, and all velocity values of each group were averaged. This phase-averaged time-resolved APV is depicted in Fig. 6 as an example for  $x = 0$  with 95 % CIs. Thereby, the time has been normalized to the acoustic period  $f_{ac}^{-1}$ . There is a good agreement of the measured data with the sinusoidal fit. Thereby, a standard uncertainty of 5.5 mm/s was achieved in average for the time-resolved APV.

### 5 Measurement application

An FM-DGV measurement at a bias flow liner was performed for the first time. Therefore, a generic bias flow liner has been used in the flow duct DUCT-R.

### 5.1 Setup

The measurement setup was similar to the one from Sect. 4.1 using a grazing flow with a Mach number of  $M_g \approx 0.1$ . However, the hard-walled measurement object was replaced by a single volume bias flow liner with 53 orifices as depicted in Fig. 7a. A bias flow through the orifices was applied having a total mass flow rate of 20 kg/h which corresponds to a Mach number of about  $M_b = 0.1$ . The bias flow was also seeded with DEHS by a second

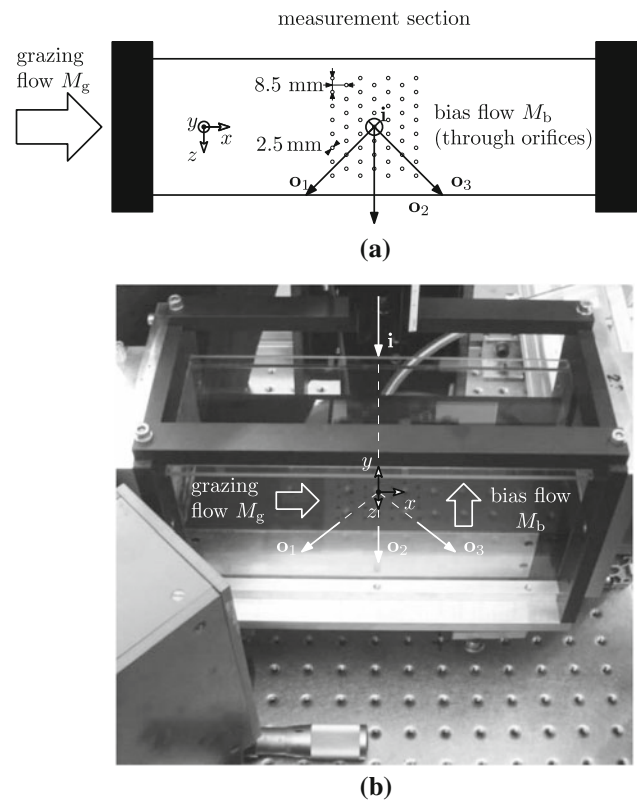


**Fig. 7** Setup of the FM-DGV measurement at this bias flow liner in the DUCT-R. **a** Liner measurement object (top view). **b** Arrangement for the sequential measurement of the three velocity components in the direction of the vectors  $(\mathbf{o}_k - \mathbf{i}), k = 1, \dots, 3$



particle generator from PIVTEC, type PivPart14. The sound was generated at an SPL of about 130 dB and a frequency  $f_{ac} = 1,073$  Hz where a high damping performance is achieved, according to preliminary investigations of the dissipation coefficient by means of microphone measurements by Heuwinkel et al. (2010).

In order to obtain three velocity components according to Sect. 2, one light incidence direction perpendicular to the liner surface and three different observation directions  $\mathbf{o}_k, k = 1, \dots, 3$  have been used sequentially, see Fig. 7b. A sequential measurement is possible since stationary conditions are assumed. This is because the acoustic frequency and the sound level of the excitation as well as the fluid temperature were not changed during the experiment. The resulting velocity components are not an orthogonal set and, thus, have to be merged using a coordinate transformation to get an orthogonal set using the procedure of Charrett et al. (2007).

To achieve a field measurement, the fibre array was orientated along the  $y$  axis and traversed along the  $x$  axis seven times with a step size of 1 mm between the measurements. The measurement duration was  $10 \times 8$  s per traversing step.

## 5.2 Results

Again, the measured APV amplitude was obtained according to Sect. 2. The resulting APV amplitude field as well as the mean flow velocity field at  $z = 0$  is depicted in Fig. 8. Here, two out of three components in the  $x$ - $y$  plane are shown. Considering the mean velocity in Fig. 8a, both the bias flow with approximately 30 m/s and the grazing flow of about 35 m/s can be identified. Some artefacts, e.g., at  $y \approx 21$  mm appear which are likely to be caused by scattered light reflected at the (uncoated) glass windows before detection resulting in a biased Doppler frequency estimation according to Fischer et al. (2011). The APV amplitude ranges from minimum 0.1 m/s at a distance of  $y = 10$  mm from the liner to maximum 2.2 m/s close to the surface of the liner ( $x = 0$  mm,  $y = 2$  mm). One has to take into consideration that this APV amplitude also comprises the deterministic portions of the flow velocity oscillation induced by the acoustic excitation, as in Heuwinkel et al. (2010). To separate both quantities, it is planned to apply the Helmholtz Hodge decomposition to the measurement data in the future. This decomposition method has been previously used in computational aeroacoustics, e.g., by De Roeck et al. (2007).

In Fig. 9, the PSD of the velocity component in the direction  $\mathbf{o}_2 - \mathbf{i}$  is depicted for different measurement points above the central liner orifice, i.e.,  $x = 0$  (Fig. 9a) and  $x = 5$  mm behind the orifice in the downstream direction (Fig. 9b). For  $y = 2$  mm, the PSD is lower

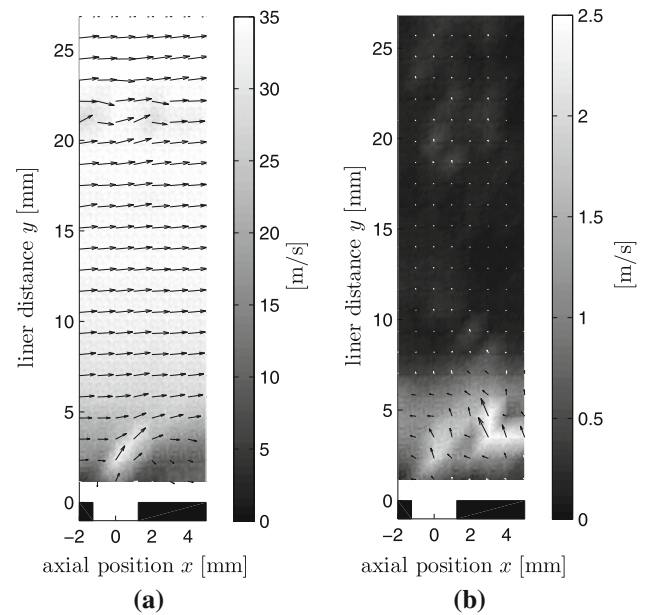


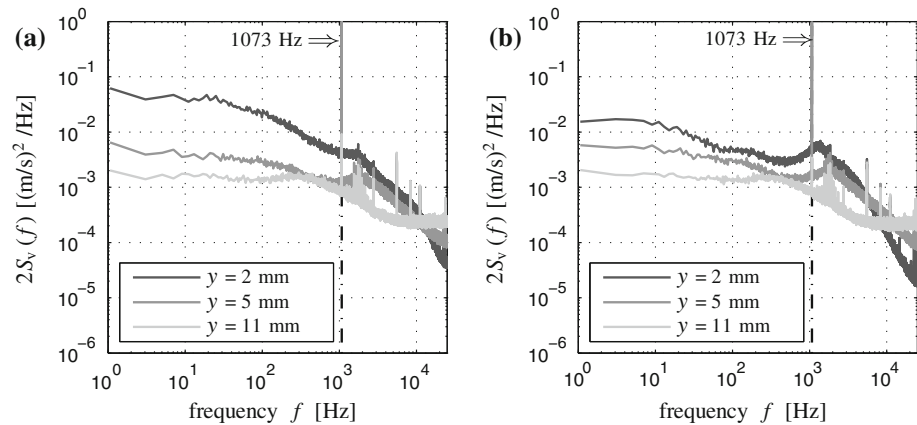
**Fig. 8** Measurement results at a bias flow liner with  $M_b = 0.1$  and  $M_g = 0.1$  at  $z = 0$ . **a** Mean velocity (in-plane). **b** APV amplitude (in-plane)

behind the orifice, especially in the frequency range below the excitation frequency  $f = 1,073$  Hz. Furthermore, the signal power obviously decreases for larger distances  $y$  to the surface of the liner in both Fig. 9a, b. The standard measurement uncertainty of the APV amplitude is about 5 mm/s in average for a measurement duration of 80 s at a measurement rate of 50 kHz. Referring to the mean flow velocity of about 35 m/s, this yields a dynamic range of about 7,000 which fits the requirements stated in Sect. 1.

## 6 Conclusions

To investigate the aeroacoustic damping phenomena of bias flow liners, simultaneous measurements of both the acoustic particle velocity field and the flow velocity field with a high dynamic range and a high measurement rate are required. For that reason, an aeroacoustic test rig was built providing a flow velocity with a maximum Mach number of 0.3. In this paper, the simultaneous measurement of the acoustic particle velocity field and the flow velocity field at a bias flow liner by means of FM-DGV was demonstrated at a Mach number of about 0.1. As a result, a high dynamic range of about 7,000 and a measurement rate of 50 kHz were achieved. The APV measurements were validated at acoustic plane waves in a flow by means of microphone measurements and showed a good agreement. In addition, velocity spectra were presented enabling the analysis of the energy transfer from the acoustic wave to turbulent

**Fig. 9** Measured PSDs of the velocity component in the direction  $\mathbf{e}_2 - \mathbf{i}$  at  $M_b \approx 0.1$ ,  $M_g \approx 0.1$  and  $z = 0$ . **a** Above orifice  $x = 0$  mm. **b** Behind orifice  $x = 5$  mm



oscillations. Time-resolved APV measurements were also shown allowing, e.g., the identification of the sound propagation direction. Future investigations will address the separation of the APV and the sound-induced flow oscillation velocity based on the obtained measurement data. Since optical methods like FM-DGV are contactless, the measurement under hot gas conditions in or near flames, for instance in combustion chambers, is also possible. To summarize, FM-DGV turns out to be a valuable tool for the analysis of damping phenomena at bias flow liners in order to reduce aircraft noise or gas turbine combustion instabilities.

**Acknowledgments** The authors thank the German Research Foundation (DFG) for sponsoring both the projects CZ55/25-1 and EN797/2-1. Many thanks go to ILA GmbH for providing the seeding particle generator. André Fischer is gratefully acknowledged for supporting the measurements.

## References

- Albrecht HE, Borys M, Damaschke N, Tropea C (2003) Laser Doppler and phase Doppler measurement techniques. Springer, Berlin
- Charrett TOH, Nobes DS, Tatam RP (2007) Investigation into the selection of viewing configurations for three-component planar Doppler velocimetry measurements. *Appl Optics* 46(19):4102–4116
- Crocker MJ (1998) Handbook of acoustics. Wiley-Interscience, New York
- De Roeck W, Baelmans M, Desmet W (2007) An Aerodynamic/Acoustic splitting technique for hybrid CAA applications. In: 15th AIAA/CEAS aeracoustics conference, Rom, Italy, 2007-3726
- Eldredge JD, Dowling AP (2003) The absorption of axial acoustic waves by a perforated liner with bias flow. *J Fluid Mech* 485(25):307–335
- European Commission (2001) European aeronautics: a vision for 2020. Office for Official Publications of the European Communities
- Fischer A, Büttner L, Czarske J, Eggert M, Grosche G, Müller H (2007) Investigation of time-resolved single detector Doppler global velocimetry using sinusoidal laser frequency modulation. *Meas Sci Technol* 18(8):2529–2545
- Fischer A, Sauvage E, Röhle I (2008) Acoustic PIV: Measurement of the acoustic particle velocity using synchronized PIV-technique. In: 14th international symposium on applications of laser techniques to fluid mechanics, Lisbon
- Fischer A, Büttner L, Czarske J, Eggert M, Müller H (2009) Measurements of velocity spectra using time-resolving Doppler global velocimetry with laser frequency modulation and a detector array. *Exp Fluids* 47(4):599–611
- Fischer A, Haufe D, Büttner L, Czarske J (2011) Scattering effects at near-wall flow measurements using Doppler global velocimetry. *Appl Optics* 50(21):4068–4082
- Haufe D, Schlüßler R, Fischer A, Büttner L, Czarske J (2012) Optical multi-point measurement of the acoustic particle velocity in a superposed flow using a spectroscopic laser technique. *Meas Sci Technol* 23(8):085306–085313
- Heuwinkel C, Fischer A, Röhle I, Enghardt L, Bake F, Piot E, Micheli F (2010) Characterization of a perforated liner by acoustic and optical measurements. In: 16th AIAA/CEAS aeracoustics conference, Stockholm, 2010-3765
- Jayatunga C, Qin Q, Sanderson V, Rubini P, You D, Krebs W (2012) Absorption of normal-incidence acoustic waves by double perforated liners of industrial gas turbine combustors. In: ASME Turbo Expo, Copenhagen, GT2012-68842
- Lahiri C, Enghardt L, Bake F, Sadig S, Gerendás M (2011) Establishment of a high quality database for the acoustic modeling of perforated liners. *J Eng Gas Turb Power* 133(9):091503–1–091503–9
- Marx D, Aurégan Y, Bailliet H, Valière JC (2010) PIV and LDV evidence of hydrodynamic instability over a liner in a duct with flow. *J Sound Vib* 329(18):3798–3812
- Minotti A, Simon F, Gantié F (2008) Characterization of an acoustic liner by means of laser Doppler velocimetry in a subsonic flow. *Aerosp Sci Technol* 12(5):398–407
- Müller H, Eggert M, Czarske J, Büttner L, Fischer A (2007) Single-camera Doppler global velocimetry based on frequency modulation techniques. *Exp Fluids* 43(2):223–232
- Raffel M, Willert C, Wereley S, Kompenhans J (1998) Particle image velocimetry: a practical guide. Springer, Berlin
- Rossing TD (2007) Handbook of acoustics. Springer, New York
- Rupp J, Carrotte J, Spencer A (2010) Interaction between the acoustic pressure fluctuations and the unsteady flow field through circular holes. *J Eng Gas Turb Power* 132(6):061501–1–061501–9
- Wang M, Freund JB, Lele SK (2006) Computational prediction of flow-generated sound. *Annu Rev Fluid Mech* 38:483–512
- Zhou G, Giannakis GB (1995) Harmonics in Multiplicative and additive noise: performance analysis of cyclic estimators. *IEEE T Signal Proces* 43(6):1445–1460